Microsyst Technol (2016) 22:129–135
DOI 10.1007/s00542-014-2358-6

TECHNICAL PAPER

Numerical study on the de-molding behavior of 2D PMMA nanochannles during hot embossing process

Zhifu Yin · Lei Sun · E. Cheng · Helin Zou

Received: 17 October 2014 / Accepted: 4 November 2014 / Published online: 13 November 2014

Abstract Hot embossing of polymethyl methacrylate (PMMA) sheet is an emerging method for fabrication of two dimensional (2D) nanochannels with low cost and high replication precision. However, the de-molding step which influences the replication precision of the final 2D PMMA nanochannels has not yet been studied systematically. In this work, the effect of the de-molding angle, de-molding temperature and friction coefficient between the 2D silicon nano-mold and the PMMA sheet on the maximum local stress in the 2D PMMA nanochannels was studied by finite element method. The results show that the maximum local stress appears in the period of 0.8–0.9 s, which indicates that the damage of 2D PMMA nanochannels may be more likely to occur at the end of the de-molding step. To separate the 2D silicon nano-mold and the PMMA sheet without nanochannels damage, the following processing parameters are suggested: de-molding angle smaller than 0.5°, de-molding temperature of 85 °C and anti-sticking treatment on the surface of the nano-mold.

1 Introduction

Nanofluidics is the analysis of the behavior, manipulation, and control of fluids which are confined to nanoscale structures (Sparreboom et al. 2009). Due to the special phenomena which only occur in nanochannels such as ultra-high surface to volume ratio and electrical double layer overlap, nanochannels become a critical method to study nano-scale fluidic, molecular and ion properties (Sparreboom et al. 2009; Freedman et al. 2013). In recent years, based on the nanochannels a great number of research has been performed, such as DNA stretching (van Kan et al. 2012; Pedersen et al. 2013), ion separation (Tsukahara 2010; Gillespie and Pennathur 2013), virus characterization (Zhou et al. 2011) and protein analysis (Anwar et al. 2012; Chun et al. 2013; Sang et al. 2013).

Hot embossing, which mainly includes heating step, pressing step and de-molding step, is a promising technology for fabrication of micro/nanostructures in polymer sheets. Comparing with conventional fabrication methods for micro/nanostructures, like ultraviolet (UV) lithography and etching processes on semiconductor substrates, hot embossing exhibits considerably better advantages in cost, resolution and productivity (Peng et al. 2013). By using this technology, high replication precision nanochannels can be fabricated in the polymer sheets. So far, sub-200 nm two-dimensional (2D) nanochannels have been replicated in the polymethyl methacrylate (PMMA), cyclic olefin copolymer (COC) and poly carbonate (PC) sheets by hot embossing techniques (Chantiwas et al. 2010; Sakamoto et al. 2011; Wu et al. 2011).

During hot embossing, it is significant to optimize the embossing parameters to replicate 2D nanochannels into the polymer sheet with high precision. The finite element method, a numerical method to find proximate solutions to boundary value problems, is a quantitative analysis technique for process optimization. By finite element method, the heating step and pressing step have been studied to increase the replication precision of the 2D polymer

Z. Yin · L. Sun · E. Cheng · H. Zou (✉)
Key Laboratory for Micro/Nano Technology and Systems of Liaoning Province, Dalian University of Technology, 116024 Dalian, People's Republic of China
e-mail: zouhl@dlut.edu.cn

H. Zou
Key Laboratory for Precision and Non-traditional Machining Technology of Ministry of Education, Dalian University of Technology, 116024 Dalian, People's Republic of China

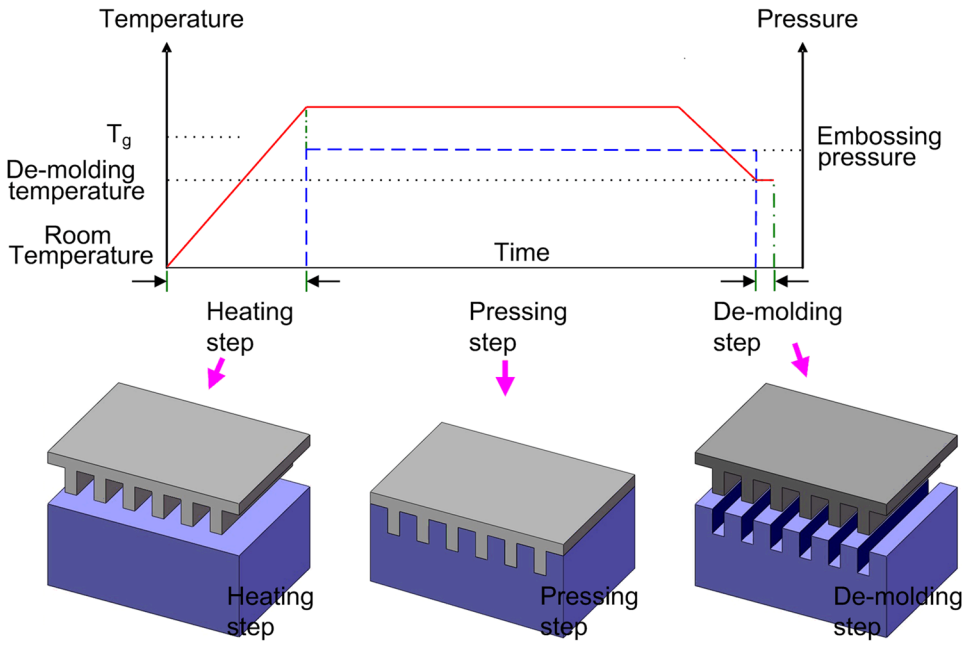

Fig. 1 Typical hot embossing process used in this paper, the *real line* represents the changes of the embossing temperature and *dotted line* presents the changes of the embossing pressure

nanochannels. The influence of the embossing temperature, embossing pressure and embossing time on the replication precision of the 2D polymer nanochannels was investigated (Hirai et al. 2007; Bum-Goo et al. 2008; Zhu et al. 2009). The effect of the duty ratio and depth-to-width ratio of the nano-mold and initial thickness of the polymer sheet on the flow behavior of the polymer was also studied (Hocheng and Nien 2006; Kim et al. 2008). Those researches are very helpful for fabricating high quality 2D polymer nanochannels. However, during hot embossing process, there are still some issues should be addressed. The de-molding step is a step in which the mold is separated from the polymer sheet after pressing step. This step is critical and has significant influence on the replication precision of the final 2D polymer nanochannels. Unfortunately, to best of our knowledge, there is no work which investigates the de-molding step by numerical simulation or experiment method during 2D polymer nanochannels fabrication. Therefore, an in-depth and systematical analysis on the de-molding step should be carried out.

In this paper, the de-molding parameters were studied by finite element method. The deformation of the 2D PMMA nanochannels during de-molding step was evaluated by the maximum local stress in PMMA nanochannels. The influence of the de-molding angle, de-molding temperature and friction coefficient between the 2D silicon nano-mold and the PMMA sheet on the maximum local stress of the 2D PMMA nanochannels was investigated. With optimized de-molding parameters, the PMMA sheet can successfully separated from the 2D silicon nano-mold without nanochannels damage. To verify the simulation method, the scanning electron microscope (SEM) profiles of 2D PMMA nanochannels de-molded under different de-molding conditions were compared.

2 Experiments

Hot embossing is a technique to fabricate low cost plastic micro/nano-structures by pressing the micro/nano-structures on the mold into the polymer sheet at proper pressure and temperature. Hot embossing mainly includes three steps. The first step is heating step, the second step is pressing step and the third step is de-molding step. The typical hot embossing process is shown in Fig. 1. In Fig. 1, the red line represents the changes of the embossing temperature and blue dotted line presents the changes of the embossing pressure.

The first step of heating step: the mold and the polymer sheet were heated to a temperature above the glass transition temperature (T_g) of the polymer. When the embossing temperature was above the T_g of the polymer, the polymer goes to a rubbery state (Guo 2004; Yin et al. 2014), the Young's modulus of the polymer is low (the polymer is very 'soft'), the micro/nano-structures on the mold can therefore be embossed into the polymer sheet easily. In this step, the embossing pressure was not applied on the mold and the polymer sheet.

The second step of pressing step: the embossing pressure was applied on the mold and the polymer sheet quickly at the embossing temperature, and then the pressure and temperature were maintained for a period of time. When the micro/nano-structures in the mold were embossed into the polymer completely, the temperature was falling down to the de-molding temperature.

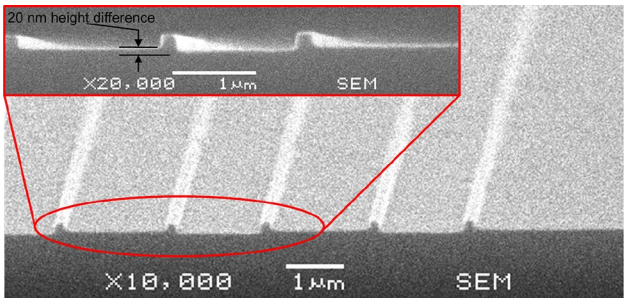

Fig. 2 SEM images of the 2D silicon nano-mold having width and height of 175 and 180 nm, respectively

The third step of de-molding step: in this step, the embossing pressure applied on the mold and the polymer sheet was released, the mold and the polymer sheet were separated. The micro/nano-structures in the mold were transferred into the polymer sheet. The de-molding temperature cannot be above the T_g of the polymer. That is because when the temperature is above the T_g of the polymer, the polymer can be reflowed after demolding step, the well embossed structure in the polymer sheet can be deformed severely (Guo 2004).

To study the influence of the demolding step on the final replication precision of the 2D PMMA nanochannels, the 0.8 mm PMMA sheets were purchased from Asahi Kasei Corporation (Tokyo, Japan) with glass T_g of 105 °C. The 0.8 mm PMMA sheet was cut into 15 mm × 15 mm square pieces. The prepared sample PMMA sheets were sonicated for 10 min in the cleaner (DZ-1, Jinan Xihua technologies Co., Ltd, Shandong, China), rinsed in the de-ionized water and dried under a nitrogen stream. Then, the hot embossing experiments can be carried out by a custom-made JHJ-I hot embossing equipment. The 2D silicon nano-mold used in this paper, shown in Fig. 2, is 175 nm wide and 180 nm high which is fabricated by the sidewall transfer technique (Rao et al. 2011). To study the de-molding step, the 2D PMMA nanochannels were de-molded at different de-molding conditions. However, during hot embossing, the conditions of heating step and pressing step were fixed at temperature of 130 °C, pressure of 2 MPa and time of 200 s.

3 Finite element methods

During the de-molding step the de-molding temperature is below the glass transition temperature of the polymer sheet. The polymer sheet is in solid state and therefore can be assumed to be an elastic body (Kim et al. 2008; Lan et al. 2009). In this paper, to simulate the de-molding step, the 2D silicon nano-mold and the PMMA sheet were considered to be elastic materials. A 2D 4-nodal linear structural element PLANE 42 was employed to represent

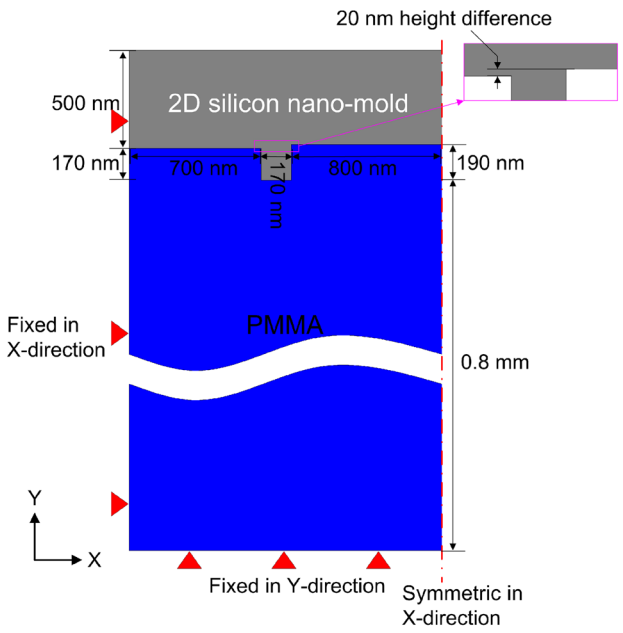

Fig. 3 Geometrical model for numerical simulation of de-molding step

the 2D silicon nano-mold and the PMMA sheet. A contact pair of CONTACT 172 and TARGET 169 was applied on the interface between the 2D silicon nano-mold and the PMMA sheet. A nonlinear finite element method software, ANSYS 10.0 (ANSYS inc., Pittsburgh, PA, USA), was employed to solve the constitutive equation and geometry equation simultaneously. For simplification, the plain-strain condition was supposed. Because the structures of the 2D silicon nano-mold were periodical, only a periodical structure was used to create the computational domain.

Figure 3 shows the geometrical model. Symmetric boundary was applied on right side of the 2D silicon nano-mold and the PMMA sheet. The *X*-axis displacement of the left side of the 2D silicon nano-mold and the PMMA sheet was set to zero due to the periodicity of the nano-features of the 2D silicon nano-mold. The *Y*-axis displacement of the bottom surface of the PMMA sheet was set to zero because the PMMA sheet was supported by a fixed hot embossing board. The 2D silicon nano-mold we used in the experiments has a 20-nm-height difference in one period (see Fig. 1). Consequently, during geometric modeling, the height difference was considered, as shown in the enlarged view of Fig. 3.

4 Results and discussions

During hot embossing process, we found that the 2D PMMA nanochannels can be easily distorted during the

de-molding step. Consequently, the deformation of the 2D PMMA nanochannels during de-molding step should be investigated. The local stress of the 2D PMMA nanochannels is a significant factor to evaluate the deformation of the 2D PMMA nanochannels. During de-molding step, when the local stress of the 2D PMMA nanochannels is larger than the yield stress of the PMMA, the unrecoverable deformation will occur. To separate the 2D silicon nano-mold and the PMMA sheet without nanochannels damage, the maximum local stress of the 2D PMMA nanochannels should be smaller than the yield stress of the PMMA. Therefore, in this paper, the deformation of the 2D PMMA nanochannels during de-molding step was estimated by the maximum local stress in 2D PMMA nanochannels. The effect of the de-molding angle, de-molding temperature and friction coefficient between the 2D silicon nano-mold and the PMMA sheet on the maximum local stress of the 2D PMMA nanochannels was analyzed by numerical simulation method. During numerical simulation, the de-molding time was set to 1 s and the 2D silicon nano-mold and the PMMA sheet were separated by applying upward displacement to the 2D silicon nano-mold.

To analyze the deformation of the 2D PMMA nanochannels during de-molding step, the yield stress of the PMMA should be taken into account. Since the yield stress of the PMMA is decreased with the increase of temperature, the yield stresses of PMMA at different temperature should be calculated or measured. The yield stress of the PMMA at different temperature can be calculated by an interpolation method according the yield stress in the reference (Quinson et al. 1997; Song et al. 2008). The yield stresses of the PMMA at different temperatures are listed in Table 1.

Table 1 The yield stress of the PMMA at different temperatures

Temp/°C	Yield stress/MPa
65	24.65
75	21.24
85	18.25
95	15.64
104	13.56

4.1 Influence of the friction coefficient

Figure 4 shows the maximum local stress of 2D PMMA nanochannels as a function of de-molding time with different friction coefficients. The effect of the friction coefficient between 2D silicon nano-mold and the PMMA sheet on the maximum local stress of the 2D PMMA nanochannels was investigated with the de-moldig temperature of 85 °C and de-molding angle of 0°. In Fig. 4, the maximum local stress increased with the increase of friction coefficient. During the whole de-molding step, the maximum local stress continuously increased from 0 to 0.8 s, and then decreased after 0.8 s. This is because from 0 to 0.8 s, the contact area between the nano-protrusion in the nano-mold and the PMMA nanochannels was decreasing, which lead to the local stress increasing. However, after 0.8 s the nano-mold and PMMA were separated. The maximum local stress of the 2D PMMA nanochannels decreases quickly within 0.2 s. The maximum local stresses were 16.78, 18.22, 19.72 and 22.22 MPa at friction coefficient of 0, 0.1, 0.2 and 0.3, respectively. It obviously that when the friction coefficient is larger than 0.2, the maximum local stress in the 2D PMMA nanochannels will be larger than the yield stress of the PMMA at 85 °C (18.25 MPa). It means that the 2D PMMA nanochannels will be destored after de-molding. In order to avoid the deformation of the 2D PMMA nanochannels, it is wise to decrease the friction coefficient between the 2D silicon nano-mold and PMMA sheet. A thin anti-sticking layer coating on the 2D silicon nano-mold is therefore suggested to decrease the friction coefficient.

4.2 Influence of the de-molding angle

The effect of the de-molding angles on maximum local stress of the 2D PMMA nanochannels during de-molding step was also investigated. Figure 5 shows the relationship between the maximum local stress and de-molding angle at friction coefficient of 0 and de-molding temperature of 85 °C. One can see that as the de-molding angle increases, the maximum local stress over the whole de-molding step increases as well. The maximum local stress increased significantly when the de-molding angle is larger than 0.5°. When the de-molding angle is larger than 0.5°, the maximum local stress in the PMMA nanochannels is much greater than the yield stress of the PMMA at 85 °C which resulting in a high degree of plastic deformation in the nanochannels after de-molding. In order to decrease the deformation of the PMMA nanochannels, the de-molding angle should be maintained below 0.5°. If possible, a zero de-molding angle is recommended.

4.3 Influence of the de-molding temperature

Figure 6 shows the maximum local stress as a function of de-molding time at different temperatures, when friction coefficient is 0 and the de-molding angle is 0°. The maximum local stress appears in the period of 0.8–0.9 s and quickly drops to zero. Contrary to the influence of the friction coefficient and the de-molding angle, the maximum local stress decreases with the increase of the de-molding temperature. In this article, the influence of the de-molding temperature on the maximum local stress above 105 °C is not discussed, because the nanochannels on PMMA sheet

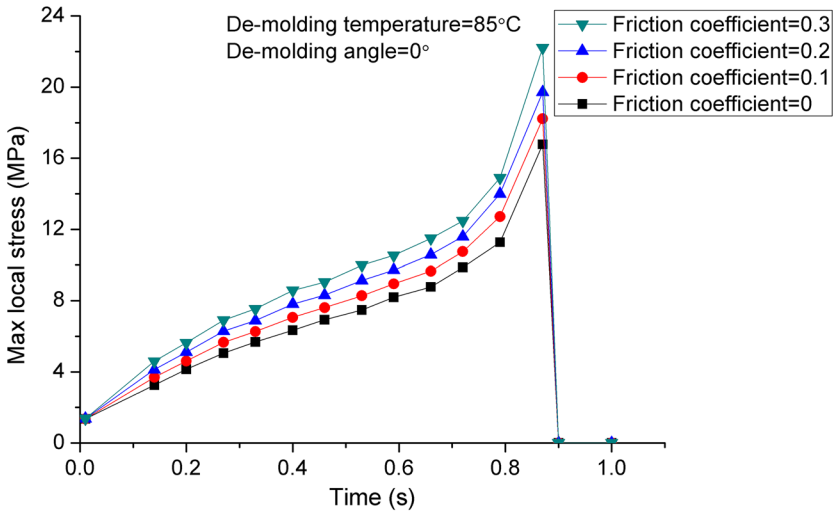

Fig. 4 The relationship between the maximum local stress and time at different friction coefficient

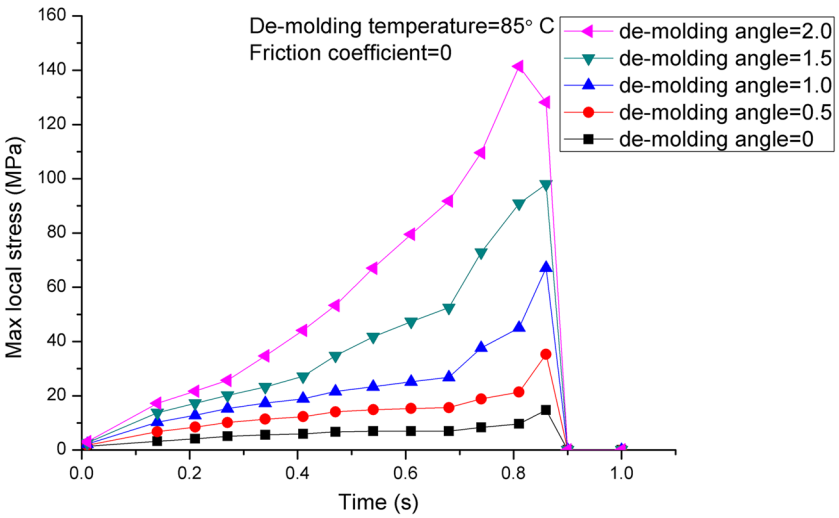

Fig. 5 Maximum local stress as a function of time at different de-molding angles

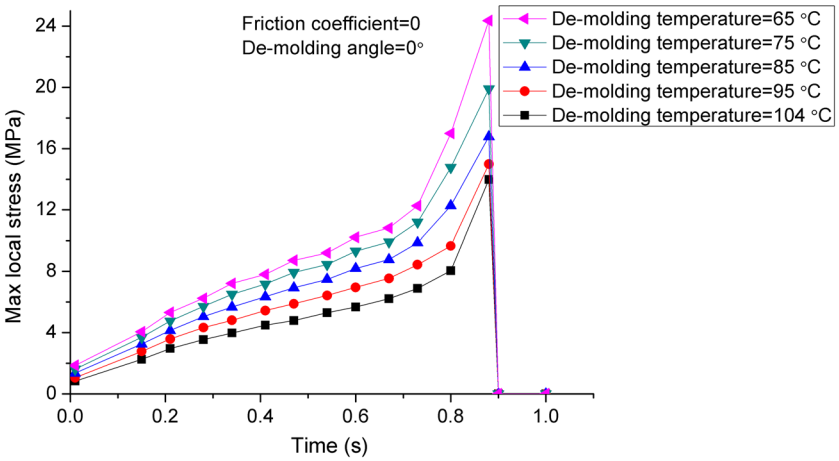

Fig. 6 Maximum local stress as a function of de-molding time at different de-molding temperatures

would be highly distorted if the de-molding temperature was higher than the glass Tg of PMMA (105 °C). By comparing of Fig. 6 with Figs. 4 and 5, we can see that the value of the maximum local stress is more significantly influenced by the de-molding angle than that by the friction coefficient and the de-molding temperature.

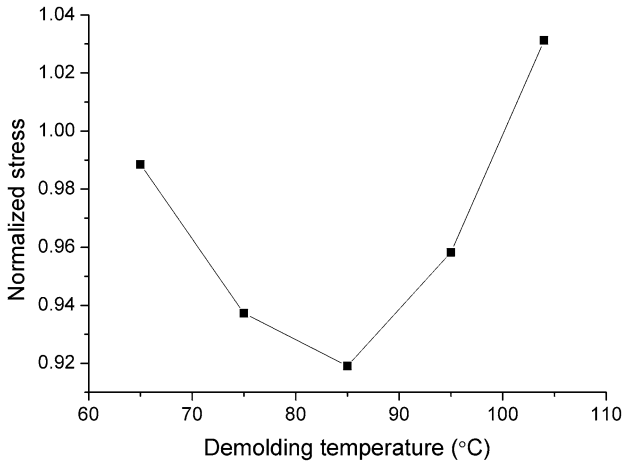

Fig. 7 Normalized stress at different de-molding temperatures

In order to investigate the deformation of the 2D PMMA nanochannels at different de-molding temperatures, the normalized stress at de-molding temperature T, $Stress_{Norm\_T}$, is defined (Eq. 1):

$$Stress_{Norm\_T} = \frac{Stress_T}{Stress_{Yield\_T}} \quad (1)$$

where, $Stress_{\_T}$ is the maximum local stress in the 2D PMMA nanochannels at demolding temperature T and the $Stress_{Yield\_T}$ is the yield stress of the PMMA at temperature T.

The normalized stress can indicate the unrecoverable deformation of the 2D PMMA nanochannels. If the maximum local stress at de-molding temperature T is larger than the yield stress of the PMMA ($Stress_{Norm\_T} > 1$), the plastic deformation in the nanochannels will occur after de-molding step. From Fig. 7 when the de-molding temperature higher than 100 °C, the 2D PMMA nanochannels will suffer plastic deformation. We can also see that the normalized stress drops first, and then increases. In order to decrease the deformation of the 2D PMMA nanochannels, we recommend choosing 85 °C as the optimized de-molding temperature.

4.4 Experimental comparison

In this paper, the 2D PMMA nanochannels were hot embossed into the 0.8 mm PMMA sheet. During heating and pressing step, the embossing parameters for replicating 2D PMMA nanochannels we chose were embossing temperature of 130 °C, embossing pressure of 2 MPa and embossing time of 200 s. In order to verify the optimized de-molding step, the 2D PMMA nanochannels were de-molded at different de-molding conditions.

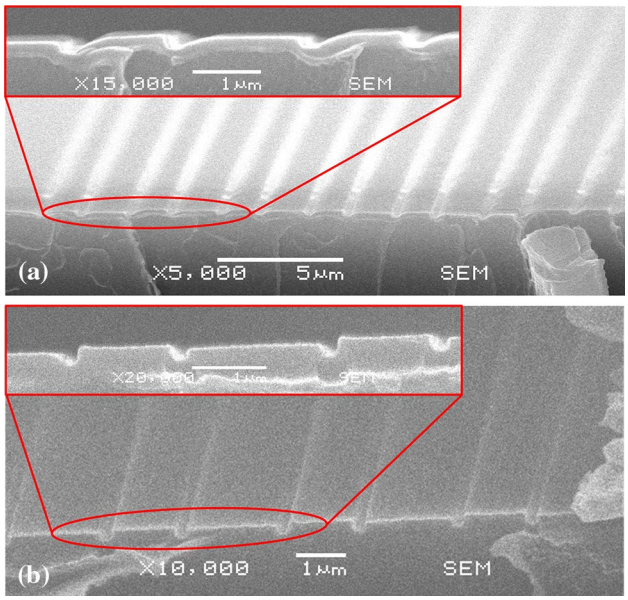

Fig. 8 SEM profiles showing 2D PMMA nanochannels after de-molding, **a** 2D PMMA nanochannels de-molded without optimized de-molding parameters, **b** 2D PMMA nanochannels de-molded with optimized de-molding parameters

Figure 8 shows SEM images of hot embossed 2D PMMA nanochannels.

The 2D PMMA nanochannels shown in Fig. 8a were de-molded at the following condition: (1) The de-molding temperature was 95 °C. (2) The PMMA sheet and the 2D silicon nano-mold were separated by hand. This means the de-molding angle was large. (3) The 2D silicon nano-mold was not treated with anti-sticking layer. This means that the friction coefficient between 2D silicon nano-mold and PMMA sheet was high.

On the other hand, the 2D PMMA nanochannels in Fig. 8b were de-molded at following the conditions: (1) The de-molding temperature was 85 °C. (2) The PMMA sheet and the nano-mold were separated vertically (de-molding angle approximately equal to 0). (3) The 2D silicon nano-mold was treated with anti-sticking layer. This means the friction coefficient between nano-mold and PMMA sheet can be considered to be 0.

From Fig. 8a and b, we can clearly see that the 2D PMMA nanochannels without the optimized de-molding parameters were highly distorted after de-molding step. However, the PMMA nanochannels de-molded under the optimized de-molding parameters stayed intact after de-molding step. It indicates that the optimized de-molding conditions obtained by the numerical simulation method can be used to fabricate high quality 2D PMMA nanochannels. The numerical simulation method is an effective way to investigate the deformation of the 2D PMMA nanochannels during de-molding step.

5 Conclusions

In this paper, the de-molding step was analyzed by numerical simulation method. The influence of the de-molding angle, de-molding temperature and friction coefficient between the 2D silicon nano-mold and the PMMA sheet on the maximum local stress of the 2D PMMA nanochannels was studied. The simulation results indicate that the impact of the de-molding angle on the maximum local stress is greater than that of the de-molding temperature and the friction coefficient. During the de-molding step, the damage of 2D PMMA nanochannels could occur at the end of de-molding step. In order to separate the 2D PMMA nanochannels from the 2D silicon nano-mold without nanochannels damage, the following processing parameters are suggested: de-molding angle smaller than 0.5°, de-molding temperature of 85 °C and anti-sticking treatment on the surface of the nano-mold.

Acknowledgments This project is supported by National Natural Science Foundation of China (No. 91023046, No. 51075059) and Specialized Research Fund for the Doctoral Program of Higher Education of China (SRFDP) (No. 20120041110034).

References

Anwar K, Han T, Kim SM (2012) An integrated micro/nanofluidic system for processing of protein samples. ASME-JSME-KSME Joint Fluids Engineering Conference (AJK2011-FED), Hamamatsu, JAPAN, American Society of Mechanical Engineers

Bum-Goo C, Soon-Yeol P, Taeyoung W (2008) Numerical simulation of on thermal nanoimprint lithography (NIL) process. 2008 In: IEEE Silicon Nanoelectronics Workshop (SNW 2008):2

Chantiwas R, Hupert ML, Pullagurla SR, Balamurugan S, Tamarit-Lopez J, Park S, Datta P, Goettert J, Cho Y-K, Soper SA (2010) Simple replication methods for producing nanoslits in thermoplastics and the transport dynamics of double-stranded DNA through these slits. Lab Chip 10(23):3255–3264

Chun D, Kim SH, Song H, Kwak S, Kim Y, Seok H, Lee S-M, Lee JH (2013) Fast myoglobin detection using nanofluidic electrokinetic trapping technique. Appl Phys Express 6(1):017001

Freedman KJ, Haq SR, Edel JB, Jemth P, Kim MJ (2013) Single molecule unfolding and stretching of protein domains inside a solid-state nanopore by electric field. Sci Rep 3:1638

Gillespie D, Pennathur S (2013) Separation of ions in nanofluidic channels with combined pressure-driven and electro-osmotic flow. Anal Chem 85(5):2991–2998

Guo LJ (2004) Recent progress in nanoimprint technology and its applications. J Phys D Appl Phys 37(11):R123–R141

Hirai Y, Onishi Y, Tanabe T, Nishihata M, Iwasaki T, Kawata H, Iriye Y (2007) Time dependent analysis of the resist deformation in thermal nanoimprint. J Vac Sci Technol B Microelectron Nanom Struct 25(6):2341–2345

Hocheng H, Nien CC (2006) Numerical analysis of effects of mold features and contact friction on cavity filling in the nanoimprinting process. J Microlith Microfab Microsys 5(1):011004

Kim NW, Kim KW, Sin H-C (2008) Finite element analysis of low temperature thermal nanoimprint lithography using a viscoelastic model. Microelectron Eng 85(9):1858–1865

Lan S, Lee HJ, Lee SH, Ni J, Lai X, Lee HW, Song JH, Lee MG (2009) Experimental and numerical study on the viscoelastic property of polycarbonate near glass transition temperature for micro thermal imprint process. Mater Des 30(9):3879–3884

Pedersen JN, Marie R, Bauer DLV, Rasmussen KH, Yusuf M, Volpi EV, Kristensen A, Mir KU, Flyvbjerg H (2013) Fully streched single DNA molecules in a nanofluidic chip show large-scale structural variation. Biophys J 104(2):175A

Peng L, Shuang P, Hao J, Qiangfei X (2013) Mold cleaning with polydimethylsiloxane for nanoimprint lithography. Nanotechnology 24(32):325301

Quinson R, Perez J, Rink M, Pavan A (1997) Yield criteria for amorphous glassy polymers. J Mater Sci 32(5):1371–1379

Rao J, Zou H, Syms RRA, Cheng E, Liu C (2011) Fabrication of 2D silicon nano-mold based on sidewall transfer. Micro Nano Lett 6(1):29–33

Sakamoto J, Fujikawa N, Nishikura N, Kawata H, Yasuda M, Hirai Y (2011) High aspect ratio fine pattern transfer using a novel mold by nanoimprint lithography. J Vac Sci Technol B 29(6):06FC15

Sang J, Du H, Wang W, Chu M, Wang Y, Li H, Zhang HA, Wu W, Li Z (2013) Protein sensing by nanofluidic crystal and its signal enhancement. Biomicrofluidics 7(2):024112

Song Z, You BH, Lee J, Park S (2008) Study on demolding temperature in thermal imprint lithography via finite element analysis, Tiergartenstrasse 17, Heidelberg, D-69121. Springer, Germany

Sparreboom W, van den Berg A, Eijkel JCT (2009) Principles and applications of nanofluidic transport. Nat Nanotechnol 4(11):713–720

Tsukahara T (2010) Nanofluidic-based separation system of radionuclide ions by controlling electrostatic forces. Bull Res Lab Nucl React 34:51

van Kan JA, Zhang C, Malar PP, van der Maarel JRC (2012) High throughput fabrication of disposable nanofluidic lab-on-chip devices for single molecule studies. Biomicrofluidics 6(3):036502

Wu J, Chantiwas R, Amirsadeghi A, Soper SA, Park S (2011) Complete plastic nanofluidic devices for DNA analysis via direct imprinting with polymer stamps. Lab Chip 11(17):2984–2989

Yin Z, Cheng E, Zou H (2014) A novel hybrid patterning technique for micro and nanochannel fabrication by integrating hot embossing and inverse UV photolithography. Lab Chip 14(9):1614–1621

Zhou K, Li L, Tan Z, Zlotnick A, Jacobson SC (2011) Characterization of hepatitis B virus capsids by resistive-pulse sensing. J Am Chem Soc 133(6):1618–1621

Zhu J, Xie H, Tang M, Li X (2009) Optimum design of processing condition and experimental investigation of grating fabrication with hot embossing lithography. Acta Mech Solida Sin 22(6):665–671